The influence of demixing on the dynamics of ionic solids: inelastic neutron scattering from $Ag_xNa_{1-x}Cl$ single crystals

2003 J. Phys.: Condens. Matter 15 6415

(http://iopscience.iop.org/0953-8984/15/37/009)

INSTITUTE OF PHYSICS PUBLISHING JOURNAL OF PHYSICS: CONDENSED MATTER

J. Phys.: Condens. Matter **15** (2003) 6415–6426 PII: S0953-8984(03)63779-3

The influence of demixing on the dynamics of ionic solids: inelastic neutron scattering from $Ag_xNa_{1-x}Cl$ single crystals

D Caspary[1], G Eckold[1], P Elter[1], H Gibhardt[1], F Güthoff[1], F Demmel[2], A Hoser[3,4], W Schmidt[2,4] and W Schweika[4]

[1] Institut für Physikalische Chemie, Universität Göttingen, Tammannstrasse 6, D-37077 Göttingen, Germany
[2] Institut Laue–Langevin, 6 rue Jules Horowitz, BP 156, F-38042 Grenoble cedex, France
[3] Institut für Kristallographie, RWTH Aachen, D-52056 Aachen, Germany
[4] Institut für Festkörperforschung, Forschungszentrum Jülich, D-52425 Jülich, Germany

Received 21 May 2003
Published 8 September 2003
Online at stacks.iop.org/JPhysCM/15/6415

Abstract

The dynamics of mixed single crystals of $Ag_xNa_{1-x}Cl$ has been investigated by inelastic neutron scattering before and after chemical demixing. In the homogeneous phase, the concentration dependence of acoustic phonons reveals that doping of NaCl with silver chloride leads to a considerable softening of the lattice, while the elastic properties of AgCl are almost independent of sodium chloride additives. After quenching into the miscibility gap, the phase separation is associated with a well-defined splitting of acoustic phonons which provide the most direct information about the underlying mechanism. In contrast to the local dynamical properties, the lattice structure is essentially determined by coherency strains which hinder the relaxation of lattice parameters. Thus diffraction and inelastic scattering yield independent and complementary information about demixing processes in ionic solids.

1. Introduction

As shown in two previous papers [1, 2], mixed ionic systems of the silver–alkali halide type are almost ideal systems for the study of demixing processes on a microscopic level. Simple phase diagrams along with large ionic mobilities and the almost rigid anion sublattice make these mixed crystals particularly suitable for kinetic investigations. Usually constituents like AgCl and NaCl or AgBr and NaBr exhibit different lattice parameters and, consequently, lattice strains play an important role during decomposition. In earlier studies [3–5], the splitting of Bragg reflections has been regarded as a tool to monitor the phase separation. From the sluggish variation of the lattice structure as reflected by changes of the Bragg profiles or the beginning opacity [6–8] it was concluded that demixing in silver–alkali halide systems takes place on a rather long timescale up to weeks or months. Recent studies using diffraction in combination

Table 1. Elastic properties of the pure compounds AgCl and NaCl at ambient temperature according to [10].

		c_{11}	c_{12}	c_{44}
AgCl	Elastic constant (GPa)	59.6	36.1	6.22
($\rho = 5.589$ g cm^{-3},	Temperature coefficient (10^{-4} K^{-1})	−10.1	−3.8	−4.28
$a = 553.9$ pm)	Pressure coefficient (10^{-12} Pa^{-1})	183	121	−81.2
NaCl	Elastic constant (GPa)	49.1	12.8	12.8
($\rho = 2.164$ g cm^{-3},	Temperature coefficient (10^{-4} K^{-1})	−7.8	4.7	−2.2
$a = 563.3$ pm)	Pressure coefficient (10^{-12} Pa^{-1})	239	183	29

with small-angle neutron scattering [1, 2], however, indicated that the phase separation appears to be much faster, within seconds or minutes. It was argued that demixing most probably takes place within an almost rigid lattice provided by the anions. The lattice relaxation is regarded as a subsequent and almost independent step in the decomposition process. Hence, diffraction alone seems to be unable to monitor the phase separation. Interestingly, the decomposition can be investigated even in single crystals without destroying the coherent lattice [9]. This observation offers the possibility for more detailed studies of the microscopic behaviour. The time evolution of phonons, in particular, can be used as the most direct probe for local interatomic interactions and their changes during demixing. Due to the limited free path of phonons these provide evidence for local properties within some 50 Å.

According to [10], the elastic constants of AgCl and NaCl differ considerably, thus offering the possibility of observing changes in local interactions and local sound velocities by inelastic neutron scattering. The elastic properties of the pure compounds are collected in table 1. In particular, the shear constant c_{44} of AgCl and NaCl differs by almost a factor of 2. Hence, the phase separation is expected to be associated with a well-defined splitting of phonon branches.

In this paper, we report on the spectra of transverse acoustic phonons in mixed crystals of AgCl–NaCl before and after demixing. This system exhibits an almost symmetrical miscibility gap with a critical temperature of about 198 °C [11]. It will be shown that phonons unambiguously prove that the phase separation and the lattice relaxation are two different aspects of decomposition.

Even the kinetics of the demixing process can be examined by time-resolved phonon experiments. The corresponding results will be presented in a subsequent paper.

2. Experimental details

Large (cm^3) single crystals of $Ag_xNa_{1-x}Cl$ were grown from the melt by the Czochralski method in an N_2 atmosphere using a ceramic crucible (FYZ Friatech) and commercially available agents (AgCl: Acros 99.9%, NaCl: Merck >99.5%). Due to the unfavourable shape of the liquidus–solidus curves, ingots were highly enriched with AgCl ($x_0 \approx 0.8$–0.9) in order to obtain single crystals with intermediate silver concentrations. Either pure NaCl crystals (Korth Kristalle GmbH) or sodium-rich fragments of preceding growth experiments with [110] orientation were used as seed crystals. Typical growth rates of less than 0.3 mm h^{-1} yielded crystals with volumes of several cubic centimetres. A typical example is shown in figure 1. In order to minimize possible concentration gradients, the crystals were annealed for about 24–48 h above 400 °C. For the determination of the actual concentration, three different small pieces were cut from the crystals along their growth direction and analysed by atomic absorption spectroscopy and by x-ray diffraction (within the homogeneous phase at 400 °C).

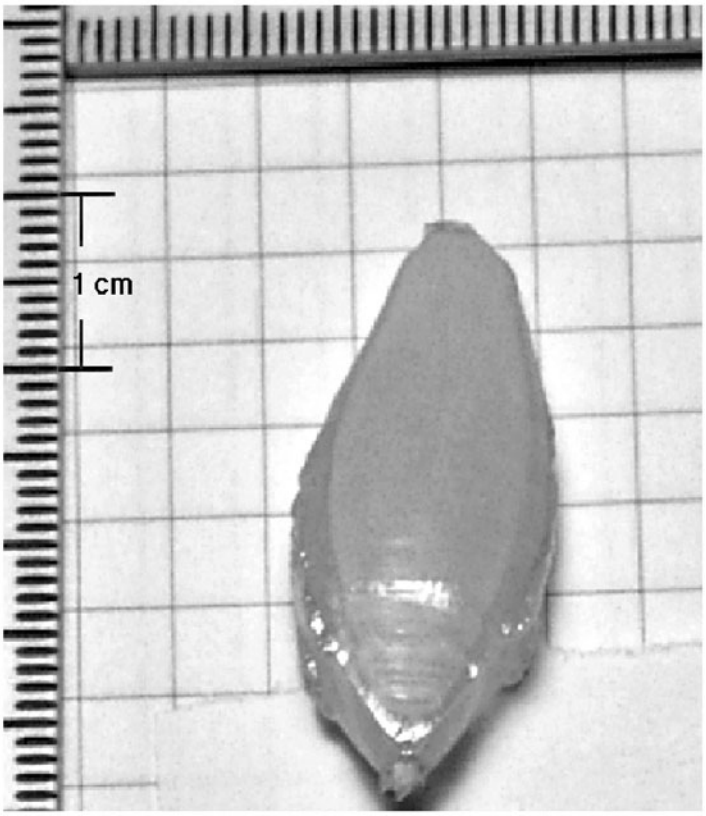

Figure 1. Single crystal of $Ag_{0.41}Na_{0.59}Cl$ as grown by the Czochralski technique.

The data prove the good homogeneity of the crystals. For the present experiments, crystals with AgCl concentrations of $x_0 = 0.23$, 0.26 and 0.41 were used. Their quality was checked by gamma-ray diffraction yielding mosaicities of less than 1°.

Specially designed furnaces were developed which were optimized for rapid cooling and heating. Details are described in [12]. The crystals were wrapped in silver foil in order to guarantee the temperature homogeneity. All experiments were performed in normal atmosphere.

The neutron scattering experiments were performed at the three axes spectrometers UNIDAS (FRJ-2, Jülich), IN3 and IN12 (HFR, ILL-Grenoble) using different combinations of neutron energy, collimation, etc. For additional diffuse elastic experiments the DNS instrument in Jülich was used.

3. Results

3.1. Acoustic phonon dispersion in the homogeneous phase

As a typical example, figure 2 shows a TA phonon along the [100] direction at 400 °C obtained for a mole fraction $x_0 = 0.41$ of silver chloride. The phonon frequency of 0.50 THz for $\mathbf{q} = (0.2\ 0\ 0)$ lies in between the values of the pure components as indicated by the arrows. The latter ($\nu_{NaCl} = 0.84$ THz and $\nu_{AgCl} = 0.35$ THz) are obtained by extrapolation from room temperature data, e.g. [13, 14], using the temperature coefficients of the elastic

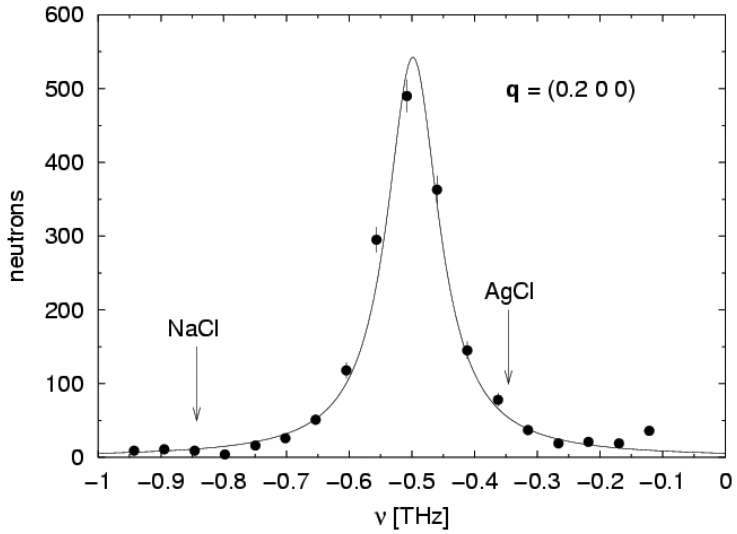

Figure 2. Typical TA phonon spectrum of an $Ag_{0.41}Na_{0.59}Cl$ mixed crystal in the homogeneous phase at 400 °C for the wavevector $\mathbf{q} = (0.2\ 0\ 0)$.

Table 2. Combinations of elastic constants as obtained by the initial slopes of the acoustic phonon branches of $Ag_xNa_{1-x}Cl$ at 330 °C.

x_0	TA[100] c_{44} (GPa)	TA[110] c_{44} (GPa)	TA[111] $c_{11} - c_{12} + c_{44}$ (GPa)	LA[100] c_{11} (GPa)	TA[110] $c_{11} + c_{12} + 2c_{44}$ (GPa)	LA[111] $c_{11} + c_{12} + 4c_{44}$ (GPa)
0.23	12.4					
0.26	11.1	11.4	39.2	62.6	110	155
0.41	8.2					

constant c_{44} (see table 1). The phonon line shape of the mixed crystal is very well represented by a Lorentzian. The line width of about 0.10 THz is only slightly larger than the experimental resolution.

Figure 3 displays the low-frequency part of the acoustic phonon branches along the main symmetry directions [100], [110] and [111] for a mixed crystal with $x_0 = 0.26$ at 330 °C. The lines represent a fit using a polynomial of order 2. From the initial slopes at $q = 0$, the elastic constants of the mixed crystal are obtained. The results are collected in table 2 along with some data for two other compositions.

For the $x_0 = 0.26$ sample, we were able to determine the whole set of three elastic constants from six different phonon branches consistently:

$$c_{11} = 58 \pm 7 \text{ GPa}$$
$$c_{12} = 29 \pm 6 \text{ GPa}$$
$$c_{44} = 11.3 \pm 0.2 \text{ GPa}.$$

For the other two concentrations, we focused our attention on the TA[100] phonon in order to determine the concentration dependence of phonon frequencies. For $\mathbf{q} = (0.3\ 0\ 0)$ the corresponding frequencies are collected in table 3.

The data of the pure compounds were obtained from the literature, e.g. [13, 14], and are extrapolated to 330 °C. The data of the $x_0 = 0.41$ sample are determined at 400 °C and

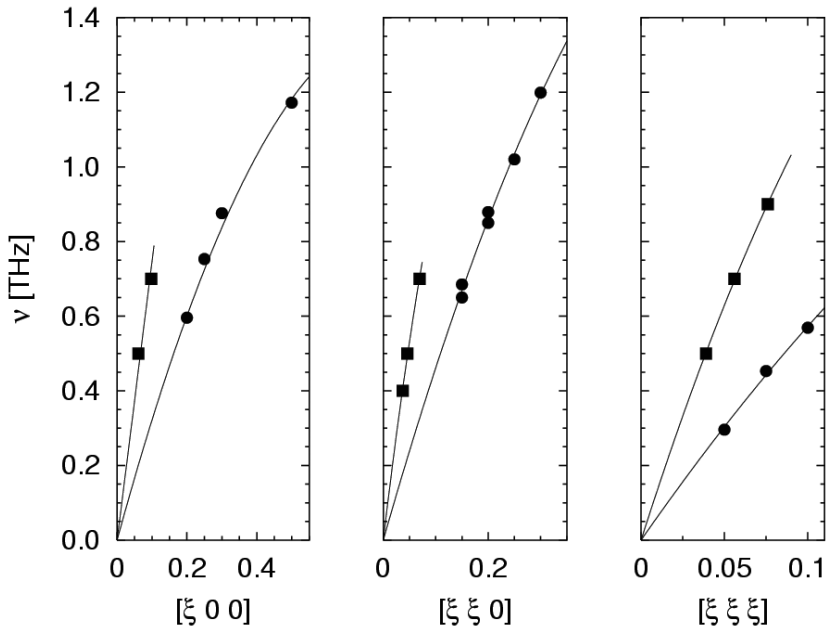

Figure 3. Dispersion of the low-energy part of transverse (●) and longitudinal (■) acoustic phonons in $Ag_{0.26}Na_{0.74}Cl$ at 330 °C along the main symmetry directions. (Note that the TA[110] phonon is polarized along [001].)

Table 3. Concentration dependence of TA phonon frequencies at 330 °C and $\mathbf{q} = (0.3\ 0\ 0)$. The experimental error is estimated as 0.03 THz.

x_0	$\nu_{TA[0.3\ 0\ 0]}$ (THz)
0	1.25
0.23	0.95
0.26	0.88
0.41	0.69
1	0.51

corrected with the help of the temperature coefficient of c_{44}. Note that the frequency shift due to the higher temperature is only about 1%, which is smaller than the experimental error of about 0.03 THz. Obviously, there is a non-linear variation of frequencies with composition. In sodium-rich mixed crystals ($x < 0.5$) the frequency changes by almost 50%, while it becomes almost independent of composition in silver-rich compounds.

3.2. Acoustic phonons in demixed crystals

After quenching to room temperature and ageing for more than six months, $Ag_xNa_{1-x}Cl$ single crystals exhibit phonon spectra as shown in figure 4 for a phonon wavevector of $\mathbf{q} = (0.2\ 0\ 0)$ and two different initial concentrations x_0. Besides an incoherent elastic peak, there are two different and well-defined phonons which are observed in neutron energy gain ($\nu < 0$) as well as in neutron energy loss ($\nu > 0$). The inelastic peak at about ± 0.41 THz is due to the TA phonon of the silver-rich phase, while the phonon of the sodium-rich phase is observed at ± 0.85 THz. The line widths of both phonons are only slightly larger than the experimental

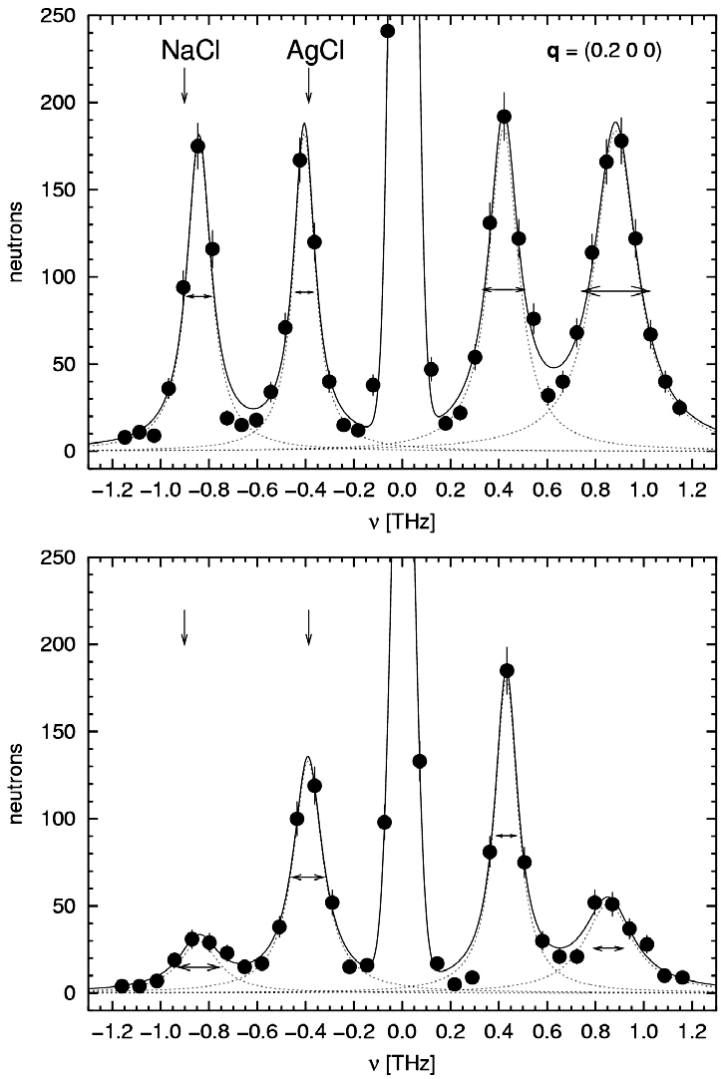

Figure 4. TA phonon spectra, $\mathbf{q} = (0.2\ 0\ 0)$, after ageing for more than six months at room temperature with $x_0 = 0.23$ (top) and $x_0 = 0.41$ (bottom). The horizontal arrows represent the experimental resolution.

resolution, thus indicating that chemical decomposition is almost completed. This finding is supported by the fact that the phonon frequencies of the product phases are independent of the initial overall concentration x_0. Inspection of figure 4 shows that spectra for $x_0 = 0.23$ and 0.41 differ only in the relative phonon intensities but not in the peak position since the concentrations of the coexisting phases (x_1 and x_2) are the same in both cases.

The ratio of the phonon intensities is given by the volume fractions and the dynamical structure factors of the corresponding phases. Neglecting differences in the Debye–Waller factors and using the high-temperature approximation ($h\nu/k_{\mathrm{B}}T \ll 1$) and the lever rule we obtain

$$\frac{I_1}{I_2} = \frac{x_2 - x_0}{x_0 - x_1}\frac{\sigma_1^{\mathrm{coh}}}{\sigma_2^{\mathrm{coh}}}\left(\frac{\nu_2}{\nu_1}\right)^2 \tag{1}$$

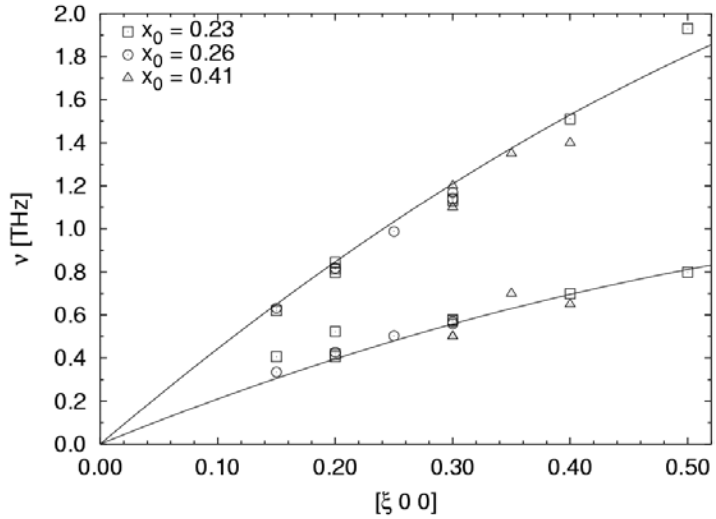

Figure 5. Dispersion of TA[100] phonons in demixed crystals of different overall compositions.

with

$$\sigma_i^{\mathrm{coh}} = 4\pi(x_i b_{\mathrm{Ag}} + (1 - x_i)b_{\mathrm{Na}} + b_{\mathrm{Cl}})^2 \tag{2}$$

where $b_{\mathrm{Ag}} = 0.592 \times 10^{-12}$ cm, $b_{\mathrm{Na}} = 0.363 \times 10^{-12}$ cm and $b_{\mathrm{Cl}} = 0.958 \times 10^{-12}$ cm are the coherent scattering lengths of the individual elements.

If one assumes that the concentrations of the product phases are given by the binodal as obtained by Sinistri *et al* [11], the two phonons correspond to $x_1 = 0.05$ and $x_2 = 0.95$, respectively. Using these data in equation (1), the intensity ratio is calculated to be 0.69 and 0.26 for the sample with $x_0 = 0.23$ and 0.41, respectively, in reasonable agreement with the data in figure 4.

The low-energy part of the TA phonon dispersion along [100] is shown in figure 5. Obviously, the results of three demixed crystals with different overall concentrations coincide for all wavevectors. This finding yields another indication that the chemical demixing is almost complete and all crystals consist of product phases with compositions close to the binodal.

After extrapolation to 330 °C, the phonon frequencies of these product phases can be used along with the data of table 3 to complete the concentration dependence of ν_{TA}. All available data are collected in figure 6 which shows that even small amounts of silver chloride introduced into the NaCl host lattice lead to a substantial softening of the lattice. Interestingly, the shape of $\nu(x)$ resembles the solidus curve as obtained by Sinistri *et al* [11]. This finding is consistent with the phenomenological ansatz introduced by Ubbelohde [15] which relates the shear module to the melting temperature.

This non-linear behaviour may be discussed on the basis of elementary lattice dynamics of the NaCl structure.

For acoustic phonons in the vicinity of the Γ-point, the polarization vectors **u** of cations and anions are identical. Moreover, the dynamical matrix which is the Fourier transform of the force constant matrix can be expanded in a power series of the wavevector **q**. The linear range of the acoustic branch can thus be described by the sound velocity:

$$\left(\frac{2\pi\nu}{q}\right)^2 = \frac{1}{M}\sum_{\kappa}\sum_{\kappa'}\sum_{l'}(\mathbf{u}\cdot\mathbf{V}_{\kappa,\kappa' l'}\cdot\mathbf{u})\cdot\frac{(\mathbf{q}\cdot\mathbf{r}_{l'})^2}{q^2} = \frac{1}{M}\sum_{\kappa}\sum_{\kappa'}\sum_{l'}(\mathbf{u}\cdot\mathbf{V}_{\kappa,\kappa' l'}\cdot\mathbf{u})\cdot z_{l'}^2. \tag{3}$$

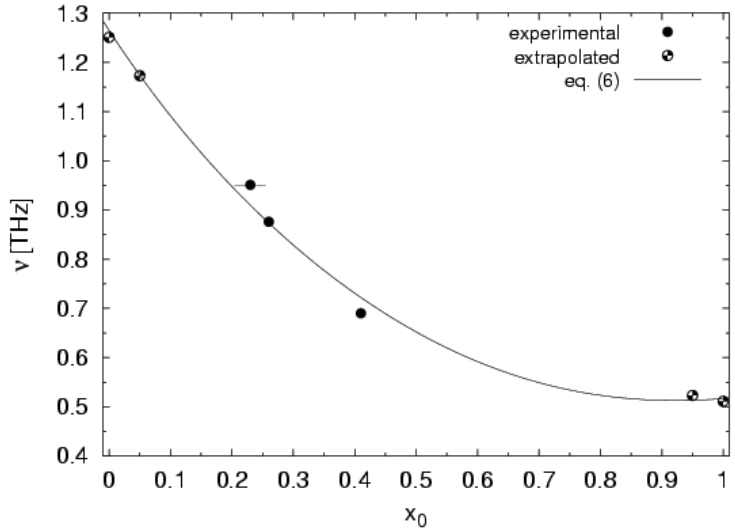

Figure 6. Concentration dependence of the TA phonon frequency at $\mathbf{q} = (0.3\ 0\ 0)$. The curve is the result of a fit to equation (6).

$\mathbf{V}_{\kappa,\kappa' l'}$ is the force constant matrix describing the interaction between particles of types κ and κ' within different primitive cells at a distance $\mathbf{r}_{l'}$, $z_{l'}$ is the component of $\mathbf{r}_{l'}$ along $\mathbf{q}$ and M is the total mass per primitive cell. In the NaCl structure, κ is + for the cation and − for the anion and, hence,

$$\left(\frac{2\pi\nu}{q}\right)^2 = \frac{1}{(m_+ + m_-)} \sum_{l'} [V_{++,l'} + 2V_{+-,l'} + V_{--,l'}] z_{l'}^2$$
$$= \frac{4}{\rho a^3} \sum_{l'} [V_{++,l'} + 2V_{+-,l'} + V_{--,l'}] z_{l'}^2. \tag{4}$$

Here, the abbreviation $V_{\pm\pm,l'} = \mathbf{u} \cdot \mathbf{V}_{\pm\pm,l'} \cdot \mathbf{u}$ is used for the projection of the force constant matrix onto the direction of polarization, while $V_c = a^3/4$ and $\rho = (m_+ + m_-)/V_c$ are the volume of the primitive cell and the density, respectively.

In a homogeneous $Ag_xNa_{1-x}Cl$ mixed crystal, silver and sodium ions are statistically distributed among the sites of the cation sublattice. Hence, we can use the mole fraction x as the occupation probability for the silver ions and obtain

$$\left(\frac{2\pi\nu}{q}\right)^2 = \left\{ \sum_{l'} [x^2 V_{\mathrm{AgAg},l'} + (1-x)^2 V_{\mathrm{NaNa},l'} + 2x(1-x) V_{\mathrm{AgNa},l'} + 2x V_{\mathrm{AgCl},l'} \right.$$
$$\left. + 2(1-x) V_{\mathrm{NaCl},l'} + V_{\mathrm{ClCl},l'}] z_{l'}^2 \right\} (x m_{\mathrm{Ag}} + (1-x) m_{\mathrm{Na}} + m_{\mathrm{Cl}})^{-1}$$
$$= \left[x^2 \sum_{l'} (V_{\mathrm{AgAg},l'} + V_{\mathrm{NaNa},l'} - 2V_{\mathrm{AgNa},l'}) z_{l'}^2 \right.$$
$$+ 2x \sum_{l'} (V_{\mathrm{AgNa},l'} - V_{\mathrm{NaNa},l'} + V_{\mathrm{AgCl},l'} - V_{\mathrm{NaCl},l'}) z_{l'}^2$$
$$\left. + \sum_{l'} (V_{\mathrm{NaNa},l'} + 2V_{\mathrm{NaCl},l'} + V_{\mathrm{ClCl},l'}) z_{l'}^2 \right] (x m_{\mathrm{Ag}} + (1-x) m_{\mathrm{Na}} + m_{\mathrm{Cl}})^{-1}. \tag{5}$$

If q is expressed in reciprocal lattice units ($q = 2\pi\xi/a$) and $z_{l'}$ is given in fractions of the lattice parameter ($z_{l'} = \alpha_{l'}a$):

$$\left(\frac{\nu}{\xi}\right)^2 = \frac{1}{(xm_{\mathrm{Ag}} + (1-x)m_{\mathrm{Na}} + m_{\mathrm{Cl}})}[-x^2(\Delta V_{\mathrm{Ag}} + \Delta V_{\mathrm{Na}}) + 2x\Delta V_{\mathrm{Ag}} + V_{\mathrm{NaCl}}]. \tag{6}$$

The quantity

$$\Delta V_{\mathrm{Ag}} = \sum_{l'} (V_{\mathrm{AgNa},l'} - V_{\mathrm{NaNa},l'} + V_{\mathrm{AgCl},l'} - V_{\mathrm{NaCl},l'})\alpha_{l'}^2 \tag{7a}$$

describes the effect of a single silver ion substituted in NaCl, while

$$\Delta V_{\mathrm{Na}} = \sum_{l'} (V_{\mathrm{NaAg},l'} - V_{\mathrm{AgAg},l'} + V_{\mathrm{NaCl},l'} - V_{\mathrm{AgCl},l'})\alpha_{l'}^2 \tag{7b}$$

is the corresponding quantity for a single sodium ion within the AgCl matrix. If we assume that the effective charges of silver and sodium ions are the same, both ΔV_{Ag} and ΔV_{Na} depend on short-range interactions only. In phenomenological models, these are usually described by a Born–Mayer potential or, more adequately, by shell models taking into account electrical polarization effects. For the lattice dynamical description of the pure compounds the reader is referred to [13] and [14].

Note that

$$\Delta V_{\mathrm{Ag}} + \Delta V_{\mathrm{Na}} = \sum_{l'} (2V_{\mathrm{AgNa},l'} - V_{\mathrm{AgAg},l'} - V_{\mathrm{NaNa},l'})\alpha_{l'}^2 \tag{7c}$$

depends on the cation–cation interactions only and is thus concerned with next nearest neighbour interactions.

The last term on the right-hand side of equation (6) is related to the elastic constant c_{NaCl} of the NaCl lattice via the relation

$$V_{\mathrm{NaCl}} = \sum_{l'} (V_{\mathrm{NaNa},l'} + 2V_{\mathrm{NaCl},l'} + V_{\mathrm{ClCl},l'})\alpha_{l'}^2 = \tfrac{1}{4}c_{\mathrm{NaCl}}a_{\mathrm{NaCl}} \tag{8a}$$

while for pure silver chloride the corresponding quantity is

$$V_{\mathrm{AgCl}} = V_{\mathrm{NaCl}} + \Delta V_{\mathrm{Ag}} - \Delta V_{\mathrm{Na}} = \tfrac{1}{4}c_{\mathrm{AgCl}}a_{\mathrm{AgCl}}. \tag{8b}$$

Inspection of figure 4 shows that the linear approximation holds for the TA[100] phonon branch up to $q = 0.3$. Hence, it is justified to fit the concentration-dependent frequency data presented in figure 6 to equation (6). The results obtained for the projection of the force constant matrix along the cubic axis are

$$\Delta V_{\mathrm{Ag}} + \Delta V_{\mathrm{Na}} = -1.71 \pm 0.31 \text{ N m}^{-1}$$
$$\Delta V_{\mathrm{Ag}} = -1.37 \pm 0.17 \text{ N m}^{-1}$$
$$V_{\mathrm{NaCl}} = 1.74 \pm 0.06 \text{ N m}^{-1}.$$

From these data the remaining quantities

$$\Delta V_{\mathrm{Na}} = -0.34 \pm 0.35 \text{ N m}^{-1}$$
$$V_{\mathrm{AgCl}} = 0.71 \pm 0.39 \text{ N m}^{-1}$$

are calculated.

Obviously, the substitution of silver ions into the NaCl host lattice has a much stronger effect (ΔV_{Ag}) than doping AgCl with sodium (ΔV_{Na}). In view of equation (7c) it is concluded that the short-range interaction between silver and sodium ions is appreciably weaker than the average of the Ag^+–Ag^+ and Na^+–Na^+ interactions.

It is probably the strong polarizability of Ag^+ which is responsible for the pronounced softening of NaCl. Silver ions are unique in their capability to occupy lattice sites with radii ranging from 0.7 to 1.3 Å [16]. Even Pauling's radius of Ag^+ (1.26 Å) is clearly larger than that of Na^+, the lattice parameters of silver and sodium halides exhibit the opposite relationship. Obviously, the deformability of the silver ion allows a flexible adaptation of its shape according to the actual surrounding. Hence, the mechanical strength of the NaCl lattice is significantly reduced by doping with silver. The pure AgCl lattice, on the other hand, seems to be able to accommodate even appreciable amounts of sodium without changing the dynamical behaviour at low frequencies.

It is clearly demonstrated that both the modification of interatomic forces with composition and the changes of the mass density lead to the non-linear behaviour of the phonon frequency and, hence, the sound velocity and elastic shear constant.

3.3. Structural properties of demixed crystals

As already shown in [1], the lattice relaxation as reflected by the splitting of Bragg reflections takes place on a much longer timescale as compared to chemical demixing. This information was inferred from the comparison of small-angle scattering and diffraction data. This finding is supported by our present single crystal experiments. Figure 7 shows the longitudinal profile of the (200) Bragg reflection obtained after more than six months. Different to the well-defined phonon spectra (figure 4) which clearly reflect the two phases of different composition, the Bragg profile consists of several broad components. Obviously, even after such a long period of time, a large fraction of the crystal exhibits the lattice parameter of the homogeneous phase as characterized by the main Bragg component near $Q = 2.016$ rlu in the $x_0 = 0.41$ sample. The beginning contraction of the silver-rich phase is reflected by the broad intensity contribution at larger wavevectors while the expansion of the sodium-rich phase leads to the component close to $\xi = 1.985$.

Note that the experimental resolution is about 0.006 rlu. Moreover, SANS experiments [1] yield that after 8 h ageing time, the precipitates exhibit typical diameters of more than 70 nm. Hence, grain size effects are unable to explain the broad Bragg reflections. Moreover, there are no indications of any diffuse scattering between the Bragg peaks which might be expected in disordered lattices.

For the overall concentration $x_0 = 0.23$, which is close to the miscibility gap at ambient temperature, the result of the continuous lattice parameter distribution is clearly seen in the lower part of figure 7.

Obviously, the silver-rich phase characterized by its low-energy phonons is formed within an anion lattice with a larger lattice parameter than expected in equilibrium. Hence, it is subjected to tensile stresses, while the sodium-rich phase is under compressive stress. On relaxation of these stresses at longer times, a shift of phonon frequencies can be expected. From the deformation $\Delta a/a$ and the elastic constants the residual stresses can be estimated to be of the order of 150 MPa. Using the pressure coefficients of c_{44} (table 1), changes in phonon frequencies of some 0.01 THz might be expected at very long times.

4. Conclusion

It has been shown that demixing processes in ionic crystals of the silver–alkali halide type can be characterized by inelastic neutron scattering from phonons in single crystals. The phase separation in AgCl–NaCl mixed single crystals is associated with the splitting of acoustic phonon branches due to the different sound velocities of the constituents. The concentration

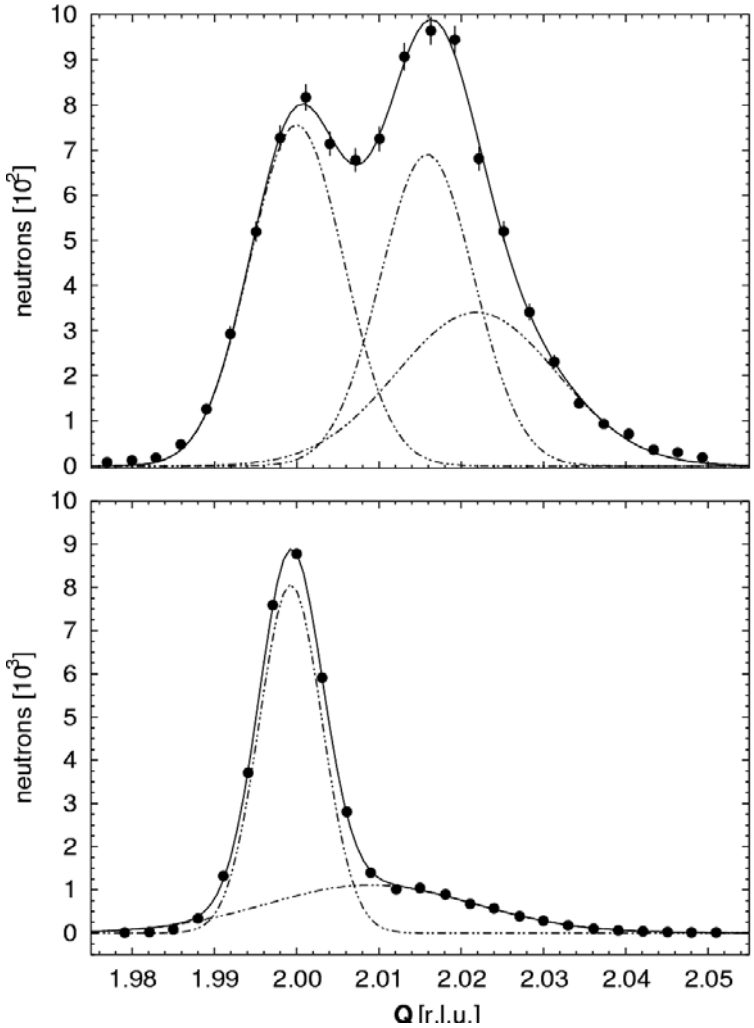

Figure 7. Longitudinal profiles of the (200) Bragg reflection for $x_0 = 0.41$ (top) and $x_0 = 0.23$ (bottom) after more than six months ageing time.

dependence of phonon frequencies and, hence, of the sound velocities and elastic constants, has been investigated in detail. It could be clearly demonstrated that not only the mass density but also the atomic interactions vary considerably with composition. Obviously, doping of NaCl with silver ions leads to a significant softening of the lattice, while the corresponding doping of AgCl with sodium ions hardly changes the elastic properties. This effect is probably due to the large polarizability of silver ions.

While phonons reflect most directly the changes of interatomic forces due to the phase separation, the static properties of the crystal lattice are essentially determined by internal coherency strains. It could be shown that the lattice relaxation is not complete even after more than six months at ambient temperature. This finding is in agreement with the results from small-angle scattering and diffraction from powder samples [1]. Interestingly, the crystal quality hardly changes even if the residual stresses after demixing are of the order of 150 MPa.

Most probably, the invariant anion sublattice acts as a rigid microscopic frame for the phase separation and prevents the destruction of single crystals.

This observation offers the possibility to study the kinetics of the demixing process via the time evolution of acoustic phonons. These investigations will provide direct evidence of the underlying mechanism and the corresponding timescale. In fact, stroboscopic studies have recently been performed. Preliminary results have been published in [16]. Details will be presented in a subsequent paper.

References

[1] Caspary D, Eckold G, Güthoff F and Pyckhout-Hintzen W 2001 *J. Phys.: Condens. Matter* **13** 11521
[2] Eckold G 2001 *J. Phys.: Condens. Matter* **13** 217
[3] Trzeciok D and Nölting J 1980 *Z. Phys. Chem. NF* **119** 183
[4] Eckold G 1992 *Jülich Report* JÜL-2675 (ISSN 0366-0885)
[5] Eckold G and Trzeciok D 1992 *Physica* B **180/181** 315
[6] Suslova V N, Shmidova N I, Zavadovskaya E K and Zvinchuk R A 1970 *Sov. Phys.—Dokl.* **15** 500
[7] Stokes R J and Li C H 1962 *Acta Metall.* **10** 535
[8] Hendricks R W, Baro R and Newkirk J B 1964 *Trans. Am. Metall. Soc. AIME* **230** 930
[9] Windgasse J, Eckold G and Güthoff F 1997 *Physica* B **234–236** 153
[10] Every A G and McCurdy A K 1992 *Landolt–Börnstein New Series* Group III, vol 29a (Berlin: Springer)
[11] Sinistri C, Riccardi R, Margheritis C and Tittarelli P 1971 *Z. Naturf.* **27**a 149
[12] Caspary D 2002 *Thesis* University of Göttingen
[13] Schmunck R E and Winder D R 1970 *J. Phys. Chem. Solids* **31** 131
[14] Vijayaraghavan P R, Nicklow R M, Smith H G and Wilkinson M K 1970 *Phys. Rev.* B **1** 4819
[15] Ubbelohde A R 1978 *The Molten State of Matter—Melting and Crystal Structure* (New York: Wiley)
[16] Elter P, Eckold G, Caspary D, Güthoff F and Hoser A 2002 *Appl. Phys.* A **74** S1179